Supporting Information:

Near-Infrared-Emitting $CuInS_2$/ZnS Dot-in-Rod Colloidal Heteronanorods by Seeded Growth

*Chenghui Xia,[a,b] Naomi Winckelmans,[c] P. Tim Prins,[a] Sara Bals,[c] Hans C. Gerritsen,[b] and Celso de Mello Donegá[a]**

a. Condensed Matter and Interfaces, Debye Institute for Nanomaterials Science, Utrecht University, P.O. Box 80000, 3508 TA Utrecht, The Netherlands

b. Molecular Biophysics, Debye Institute for Nanomaterials Science, Utrecht University, 3508 TA Utrecht, The Netherlands

c. EMAT-University of Antwerp, Groenenborgerlaan 171, B-2020 Antwerp, Belgium

*Corresponding author: E-mail: c.demello-donega@uu.nl

(1) Role of coordinating ligands

Table S1. Different coordinating ligands (2 mmol) were used in combination with $Zn(oleate)_2$ (0.25 mmol/g) for seeded injection of CIS NC seeds and S/ODE.

	$Zn(oleate)_2$	Coordinating Ligands	ODE
1	0.2 g, 0.05 mmol	--	4 ml
2	0.2 g, 0.05 mmol	707 µl, oleic acid (OA)	3.293 ml
3	0.2 g, 0.05 mmol	940 µl, oleylamine (OLAM)	3.060 ml
4	0.2 g, 0.05 mmol	892 µl, trioctylamine (TOA)	3.108 ml
5	0.2 g, 0.05 mmol	690 µl, hexadecylamine (HAD)	3.370 ml
6	0.2 g, 0.05 mmol	489 µl, 1-dodecanethiol (DDT)	3.511 ml
7	0.2 g, 0.05 mmol	991 µl, trioctylphosphine (TOP)	3.009 ml
8	0.2 g, 0.05 mmol	976 µl, trioctylphosphine oxide (TOPO)	3.024 ml

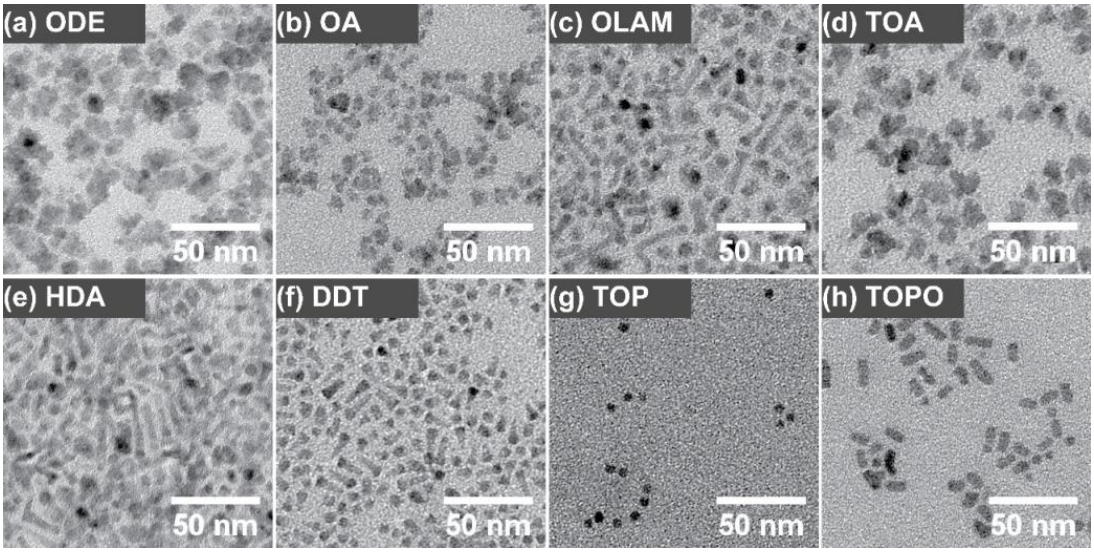

Figure S1. TEM images of the CIS/ZnS HNCs samples obtained from the seeded injection syntheses summarized in Table S1.

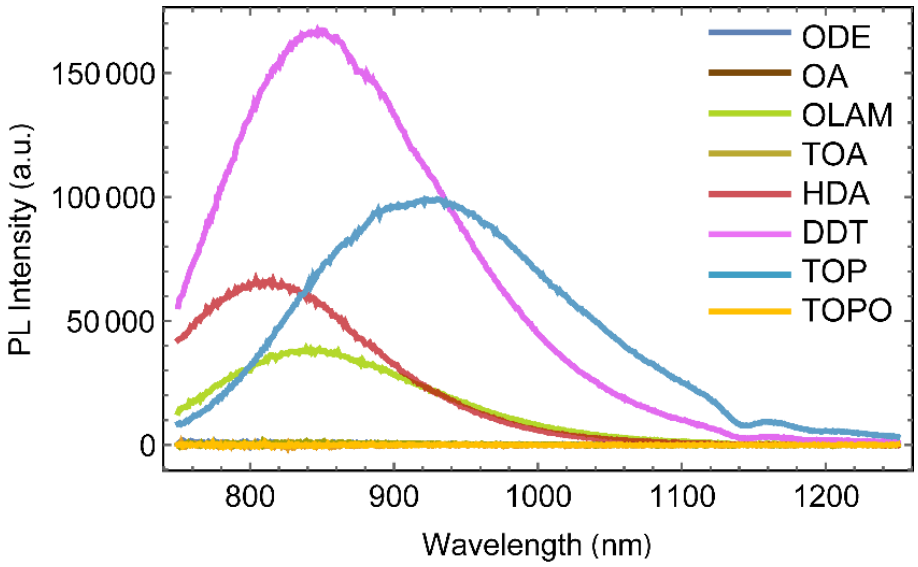

Figure S2. Photoluminescence (PL) spectra of CIS/ZnS HNCs samples obtained from the seeded injection syntheses summarized in Table S1. TEM images of these samples are shown in Figure S1. Samples for PL spectra measurements (excited at 470 nm) were prepared by diluting 300 µl of the crude reaction mixture into 3 ml anhydrous toluene.

(2) Injection sequence

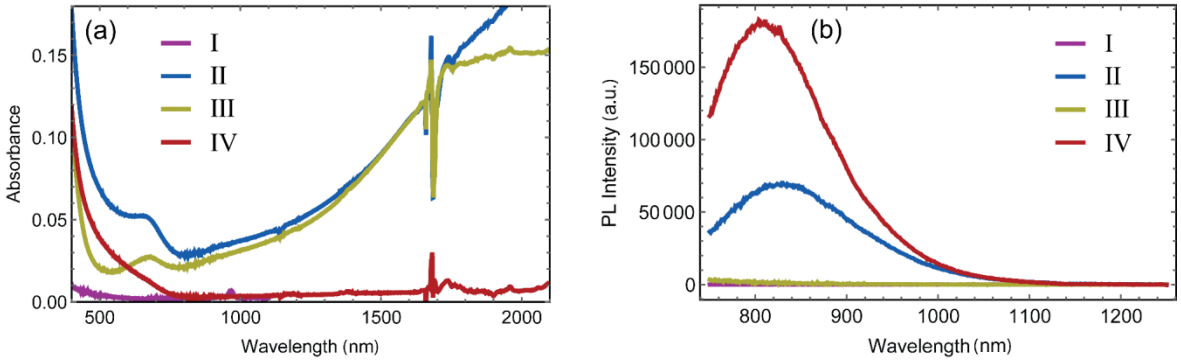

Figure S3. Absorption **(a)** and PL **(b)** spectra of the reaction products obtained from the four different seeded injection methods schematically depicted in Figure 2 of the main text. TEM images of these samples are shown in Figure 2. Samples for absorption and PL spectra measurements (excitation at 470 nm) were prepared by diluting 300 µl of the crude reaction mixture into 3 ml anhydrous toluene.

(3) Injection interval time

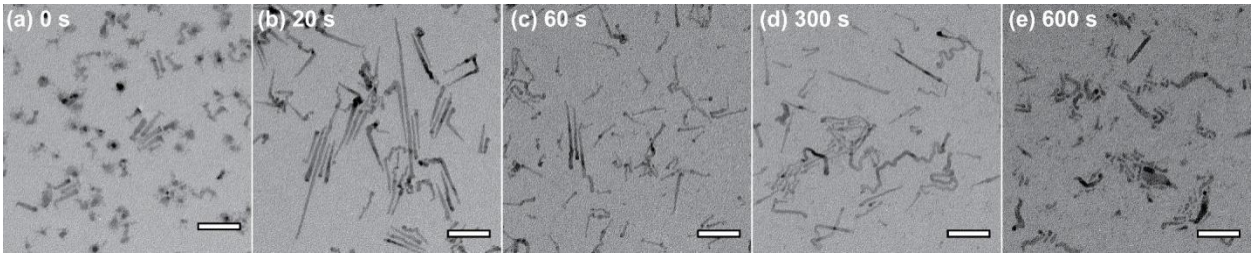

Figure S4. TEM images of CIS/ZnS HNCs synthesized by injecting S/ODE and CIS seed NCs into a solution of $Zn(oleate)_2$ and HDA in ODE at 210 °C, using injection method IV with variable injection interval times. The reaction time was 10 min. The scale bar is 50 nm.

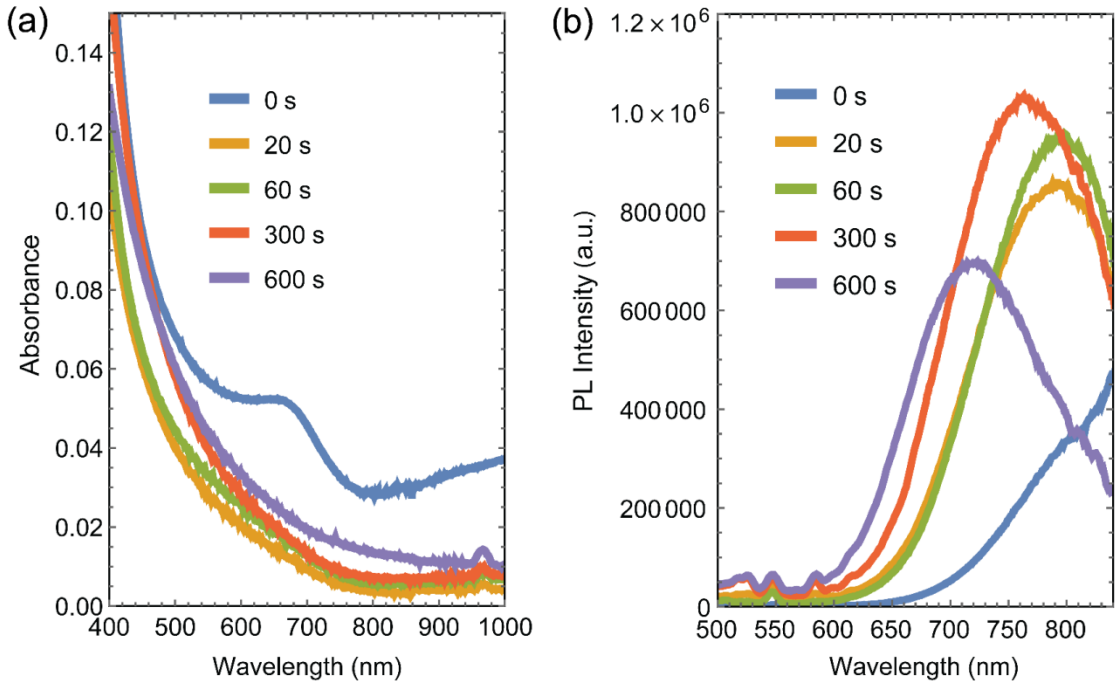

Figure S5. Absorption **(a)** and PL **(b)** spectra of CIS/ZnS HNCs synthesized by injecting S/ODE and CIS seed NCs into a solution of $Zn(oleate)_2$ and HDA in ODE at 210 °C, using injection method IV with variable injection interval times. The reaction time was 10 min. TEM images of these samples are shown in Figure S4. Samples for optical spectra measurements were prepared by diluting 300 µl of the crude reaction mixture into 3 ml anhydrous toluene.

(4) Zn/S ratio

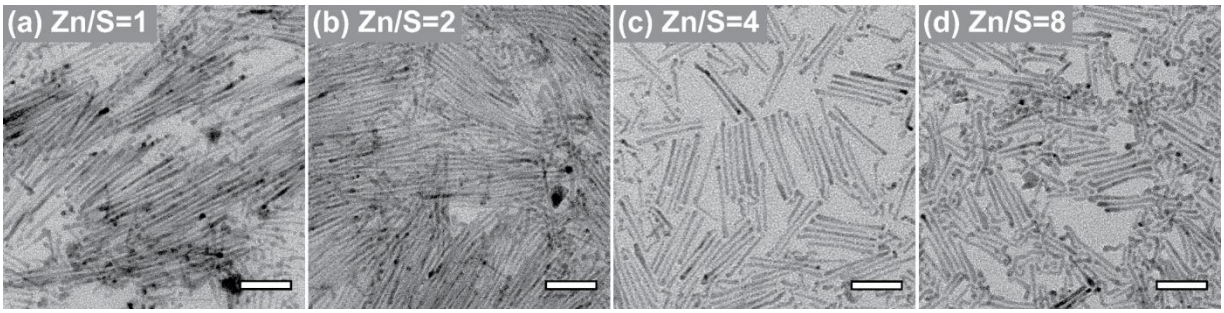

Figure S6. TEM images of CIS/ZnS HNCs synthesized by injecting S/ODE and CIS seed NCs into a solution of $Zn(oleate)_2$ and HDA in ODE at 210 °C, using injection method IV with injection interval time of 20 s and variable Zn/S ratios. The reaction time was 10 min. The scale bar is 50 nm.

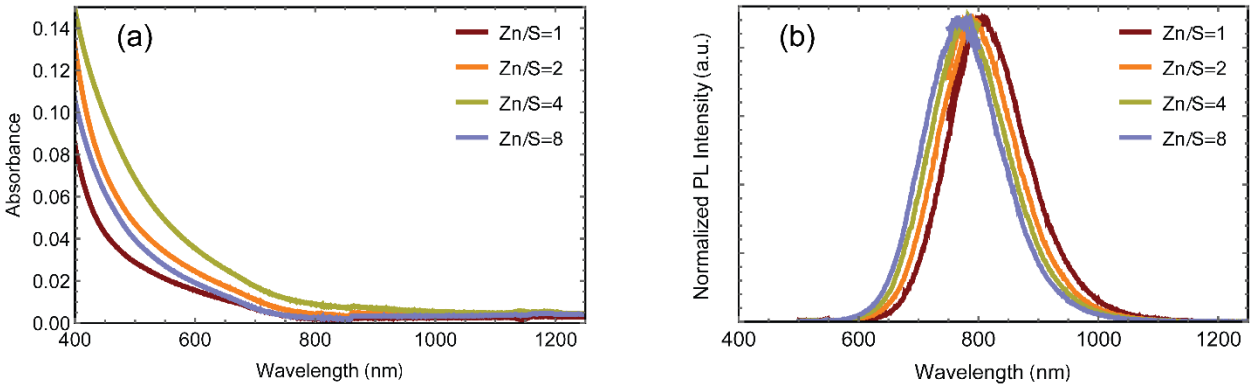

Figure S7. Absorption **(a)** and PL **(b)** spectra of CIS/ZnS HNCs synthesized by injecting S/ODE and CIS seed NCs into a solution of $Zn(oleate)_2$ and HDA in ODE at 210 °C, using injection method IV with injection interval time of 20 s and variable Zn/S ratios. The reaction time was 10 min. TEM images of these samples are shown in Figure S6. Samples for optical spectra measurements were prepared by diluting 300 µl of the crude reaction mixture into 3 ml anhydrous toluene. As the emission of CIS/ZnS NRs (~800 nm) stands at the edges of UV-Vis and NIR detector, the full PL spectra were acquired by combination of two detectors.

(5) Reaction temperature

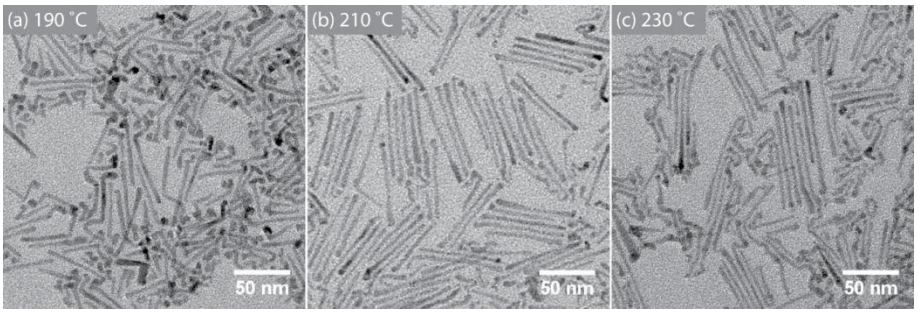

Figure S8. TEM images of CIS/ZnS HNCs synthesized by injecting S/ODE and CIS seed NCs into a solution of Zn(oleate)$_2$ and HDA in ODE at different reaction temperatures, using injection method IV with injection interval time of 20 s and Zn/S= 4. The reaction time was 10 min.

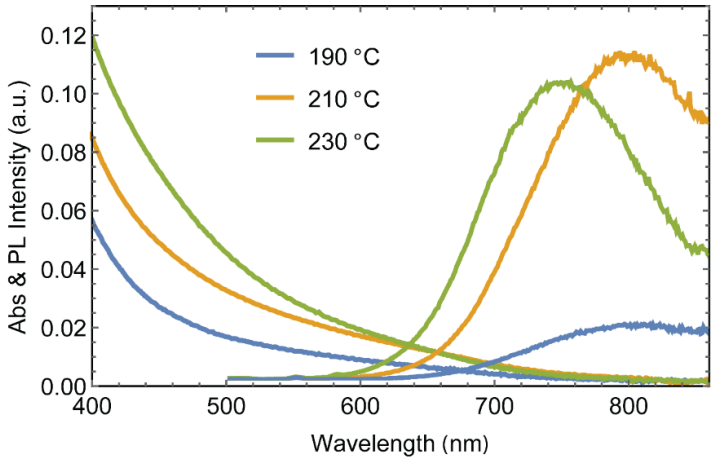

Figure S9. Absorption and PL spectra of CIS/ZnS HNCs synthesized by injecting S/ODE and CIS seed NCs into a solution of Zn(oleate)$_2$ and HDA in ODE at different reaction temperatures, using injection method IV with injection interval time of 20 s and Zn/S= 4. The reaction time was 10 min. TEM images of these samples are shown in Figure S8. Samples for absorption and PL spectra measurements (excitation at 470 nm) were prepared by diluting 300 μl of the crude reaction mixture into 3 ml anhydrous toluene.

(6) Reaction time

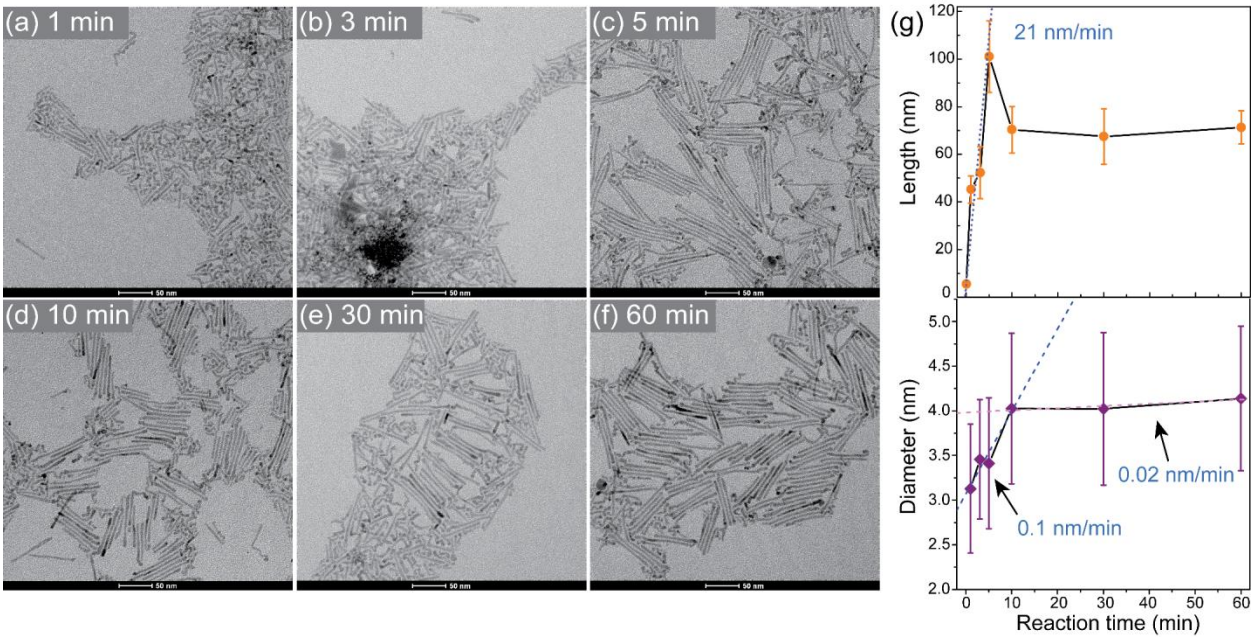

Figure S10. (a-f) TEM images of CIS/ZnS HNCs synthesized by injecting S/ODE and CIS seed NCs into a solution of $Zn(oleate)_2$ and HDA in ODE at 210 °C, using injection method IV with injection interval time of 20 s and Zn/S= 4. The reaction time was varied from 1 to 60 min. **(g)** Dimensions of the product CIS/ZnS HNCs as a function of the reaction time. The dashed line indicates the growth rate of CIS/ZnS HNCs in length and diameter.

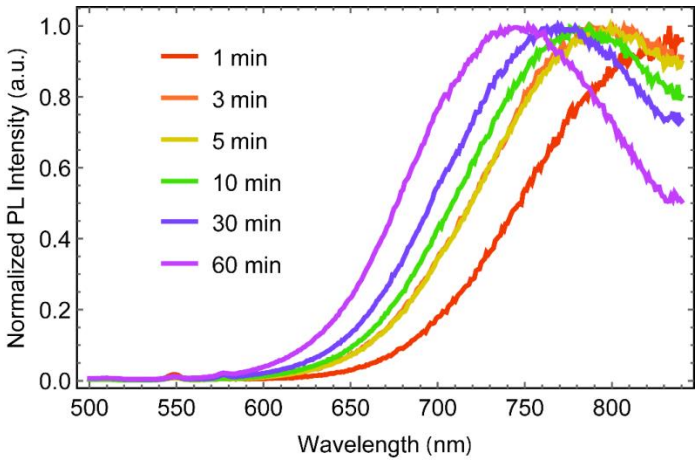

Figure S11. PL spectra of CIS/ZnS HNCs synthesized by injecting S/ODE and CIS seed NCs into a solution of $Zn(oleate)_2$ and HDA in ODE at 210 °C, using injection method IV with injection interval time of 20 s, Zn/S= 4, and reaction time from 1 to 60 min. TEM images of these samples are shown in Figure S10. Samples for absorption and PL spectra measurements (excitation at 470 nm) were prepared by diluting 300 µl of the crude reaction mixture into 3 ml anhydrous toluene.

(7) Composition of the CIS seed NCs

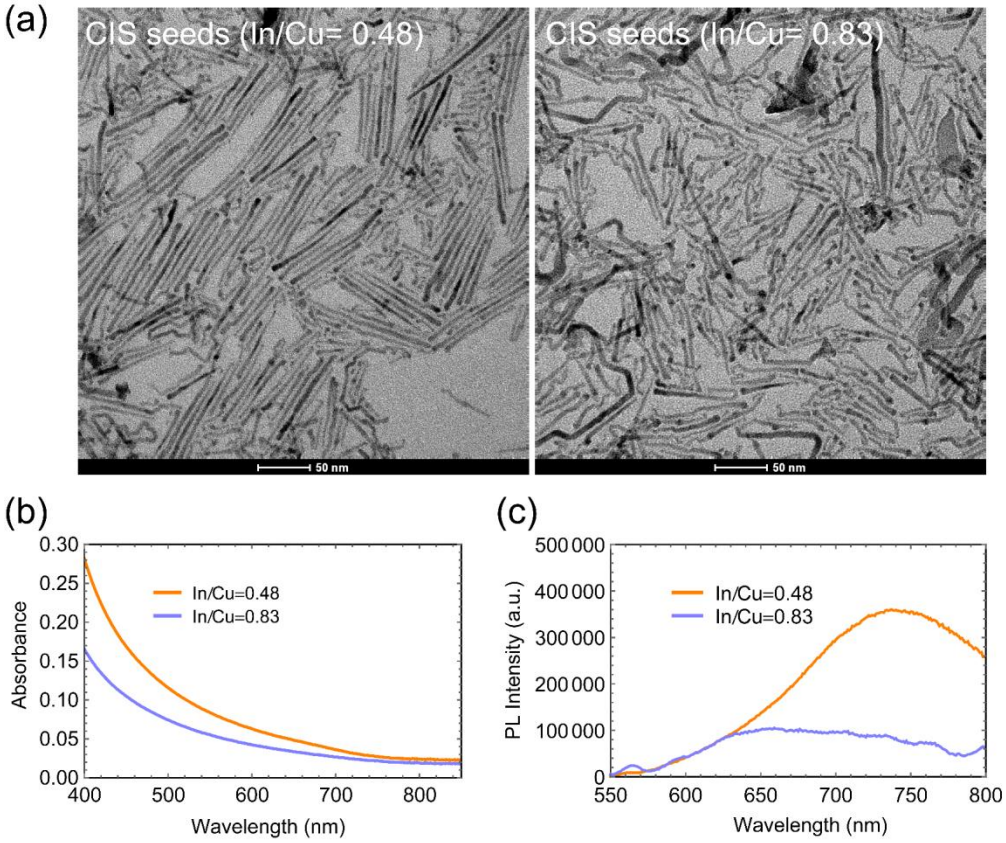

Figure S12. (a) TEM images of CIS/ZnS HNCs obtained by injection of wurtzite CIS seed NCs with two different compositions (left: In/Cu= 0.48, right: In/Cu= 0.83) and S/ODE into a solution of $Zn(oleate)_2$ and HDA in ODE at 210 ˚C following injection protocol IV. **(b-c)** Absorption and PL spectra of CIS/ZnS HNCs shown in (a). The different CIS seed NCs were obtained by room temperature Cu^+ for In^{3+} cation exchange in the same batch of template $Cu_{2-x}S$ NCs, using the same conditions (see Experimental Section in the main text for details), except for the reaction time (3 and 7 days for the In/Cu= 0.48 and 0.83, respectively).

(8) Up-scale synthesis

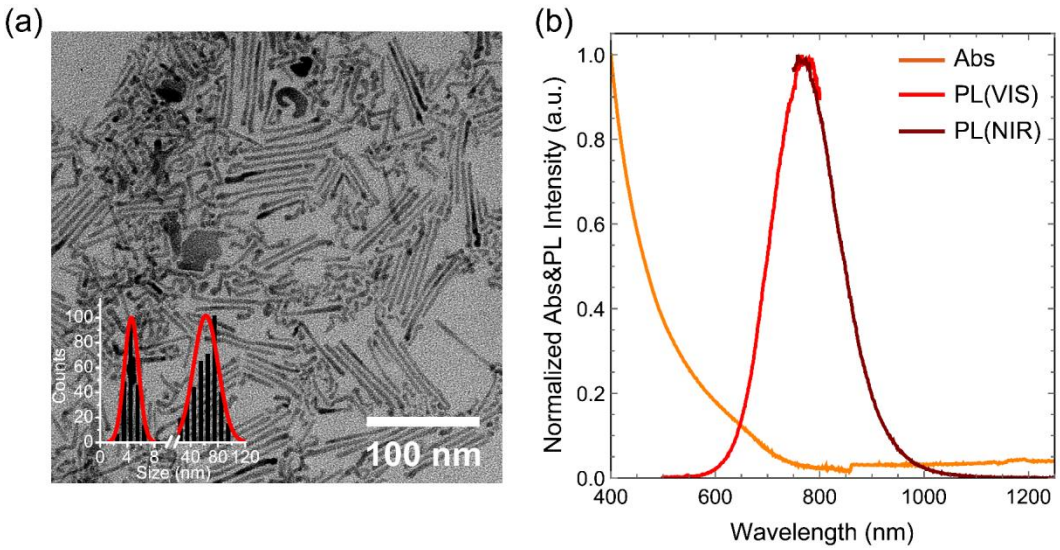

Figure S13. (a) TEM image and corresponding size histogram of CIS/ZnS HNCs prepared by injection of wurtzite CIS NC seeds and S/ODE into a solution of $Zn(oleate)_2$ and HDA in ODE at 210 ˚C following injection protocol IV. The size histograms were constructed by measuring the diameter (4.6 nm with a polydispersity of 21.7%) and length (62.3 nm with a polydispersity of 28.9%) of over 200 HNCs and are independently fitted to Gaussian distribution functions. **(b)** Absorption and PL spectra of the product CIS/ZnS HNCs obtained by seeded injection, shown in (a). As the emission of CIS/ZnS HNCs (765 nm) is at the limit of both the UV-Vis and the NIR detector, the full PL spectra were acquired by a combination of the two detectors (excitation wavelength 450 nm).

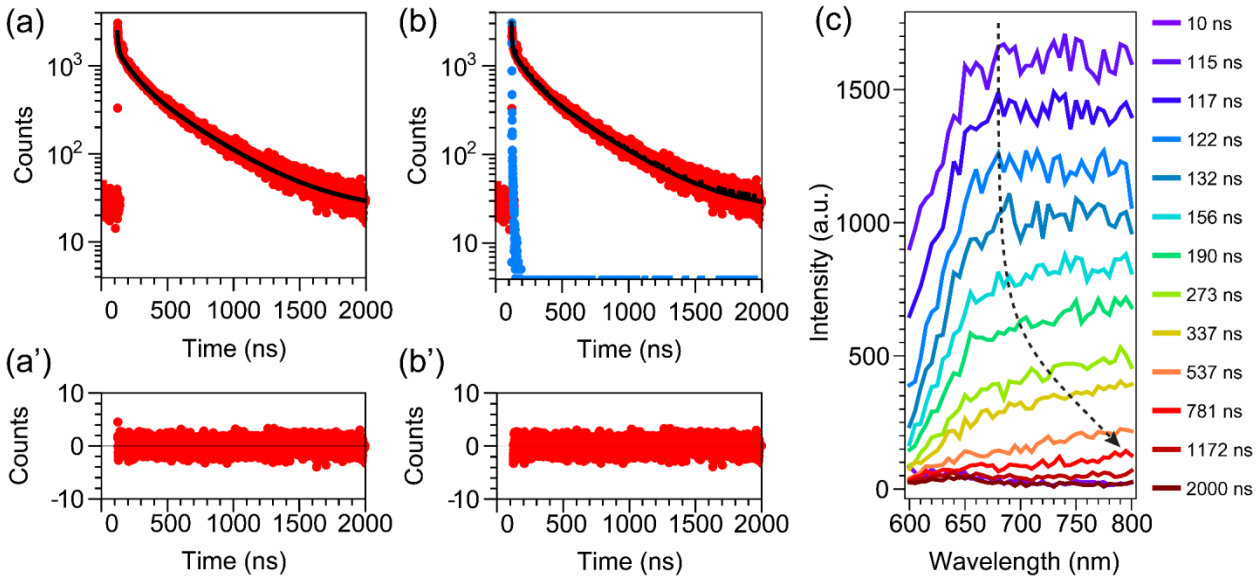

Figure S14. (a) PL decay curve of the CIS/ZnS HNCs shown in Figure 3a in the main text. The data is best fit by a triple exponential (τ_1=7.5 ns (1.8%), τ_2=107 ns (19.0%), τ_3=410 ns (79.2%)) with χ^2= 1.080 and the residuals shown in **a'**. **(b)** PL decay curve of the CIS/ZnS HNCs shown in Figure 3a in the main text and corresponding Instrument Response Function (IRF). A triple exponential fitting with deconvolution results in three decay components (τ_1=1.2 ns (13.6%), τ_2=104 ns (16.8%), τ_3=408 ns (69.6%)) with χ^2= 1.092 and the residuals shown in **b'**. The detected wavelength was set at 780 nm. **(c)** Time-resolved emission spectra of the CIS/ZnS HNCs shown in Figure 3a in the main text. The detected wavelengths were set from 600 to 800 nm with a step of 5 nm.

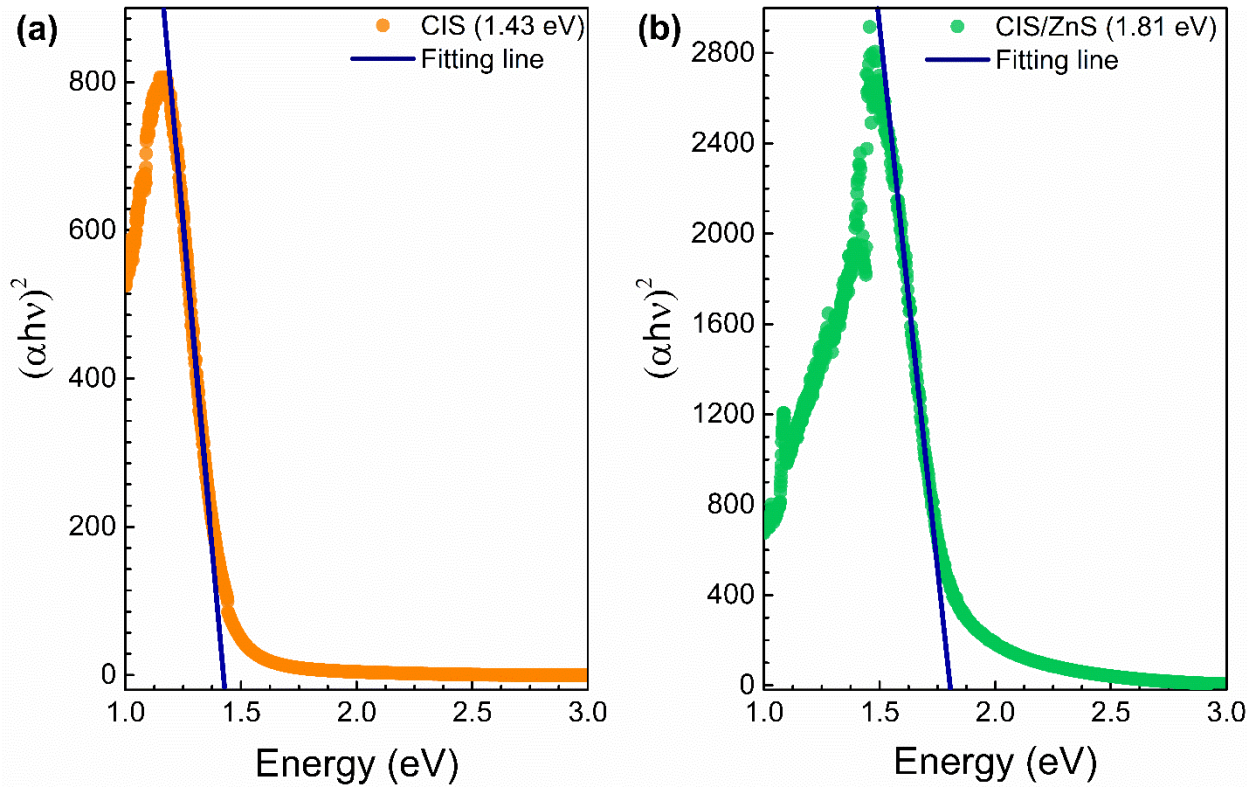

Figure S15. Experimental band gap estimation of **(a)** CIS NC seeds and **(b)** CIS/ZnS HNCs using a Tauc plot. The absorption coefficient of wurtzite $CuInS_2$ is not well known, so an approximation of the Tauc relationship for direct band-gap semiconductors was used:[1] $(\alpha h\nu)^2 = [h\nu*(1-Abs)^2/2Abs]^2$.

[1] X. Lu, Z. Zhuang, Q. Peng, Y. Li, *Chem. Commun.* **2011**, 47, 3141–3143.

Table S2. ICP analysis of $Cu_{2-x}S$, CIS and CIS/ZnS nanorods.

	In/Cu	S/Cu	Zn/Cu	Formula
$Cu_{2-x}S$	***	0.49	***	$Cu_{2.03}S$
CIS	0.48	1.23	***	$Cu_{1.63}In_{0.79}S_2$
CIS/ZnS	0.43	11.72	14.18	$(Cu_{1.73}In_{0.73}S_2)_{0.15}(ZnS)_{2.7}Zn_{0.9}$

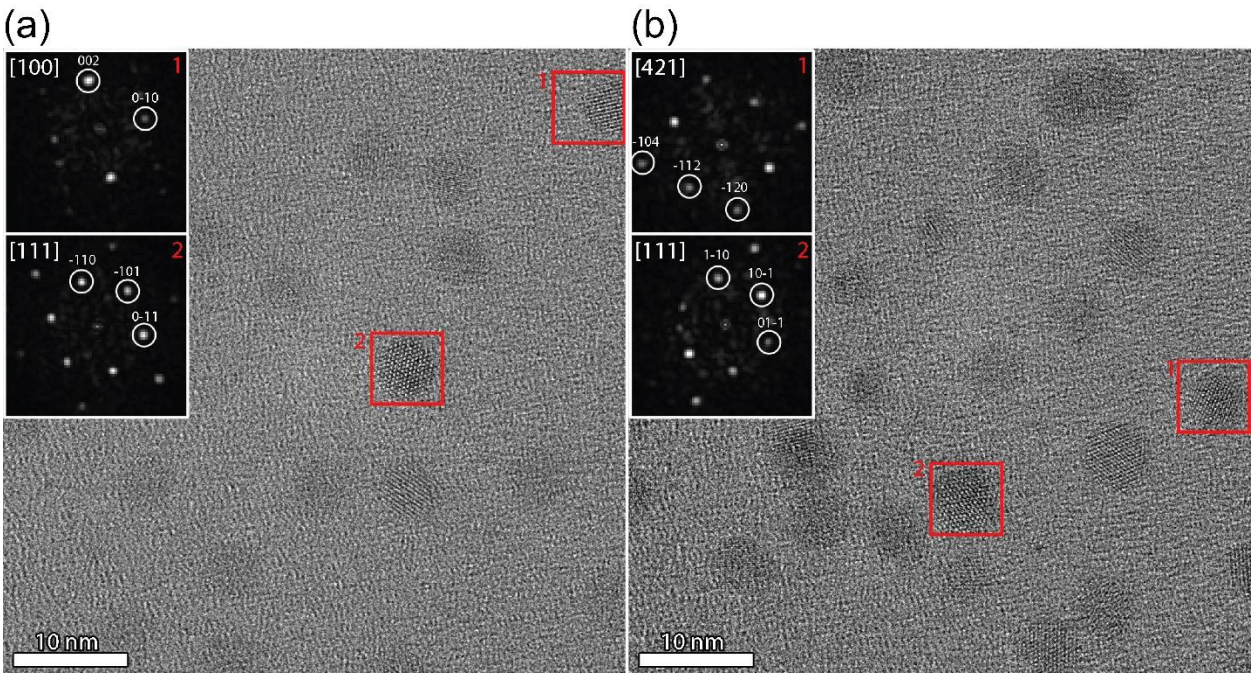

Figure S16. (a-b) High resolution TEM images and diffractograms of CIS NCs. **(a)** High resolution TEM image and diffractograms of the regions indicated with red squares. For the first diffractogram, the distances from the center to (002) and (0-10) are equal to 3.46 Å and 3.23 Å, respectively, and the angle between them is 90°, which is in agreement with the [100] zone axis of wurtzite. For the second diffractogram, the distance from the center to (-110) is equal to 3.42 Å. The angle between (-110) and (-101) is 63° and the angle between (-101) and (0-11) is 53°, which is in agreement with the [111] zone axis of wurtzite. **(b)** High resolution TEM image and diffractograms of the regions indicated with red squares. For the first diffractogram, the distance from the center to (-110) is equal to 3.42 Å. The angle between (-110) and (-101) is equal to 63° and the angle between (-101) and (0-11) is 53°, which is in agreement with the [111] zone axis of wurtzite. For the second diffractogram, the distances between the center to (1-20), (0-12) and (-104) are equal to 2.14 Å, 2.73 Å and 1.81 Å. The angle between (1-20) and (0-12) is equal to 52° and the angle between (0-12) and (-104) is equal to 38°, which is in agreement with the [421] zone axis of wurtzite.

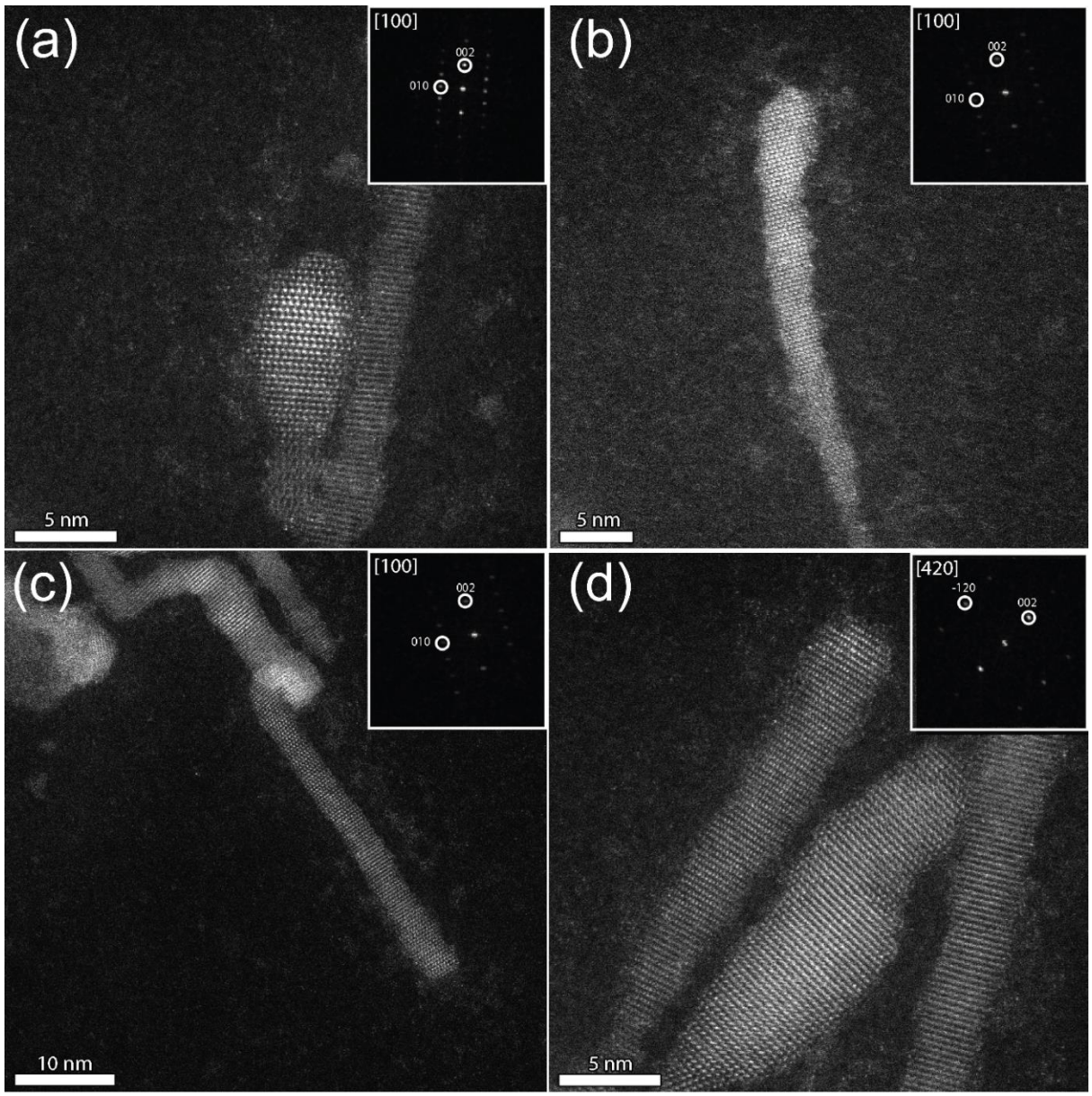

Figure S17. High-resolution HAADF-STEM image of the CIS-ZnS HNCs. Fourier transform analysis of the ZnS nanorods shows that they inherited the wurtzite structure of the CIS NC seeds, confirming the heteroepitaxial nature of the growth.

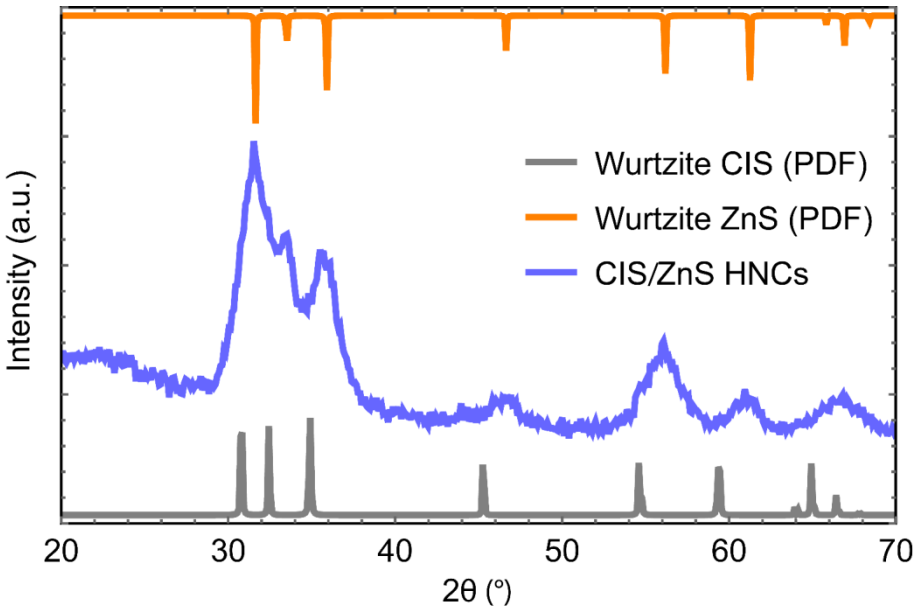

Figure S18. XRD patterns of CIS/ZnS HNCs (blue line). The gray line indicates the wurtzite CIS diffraction pattern (JCPDS Card 01-077-9459). The orange line indicates the wurtzite ZnS diffraction pattern (JCPDS Card 01-084-3995).

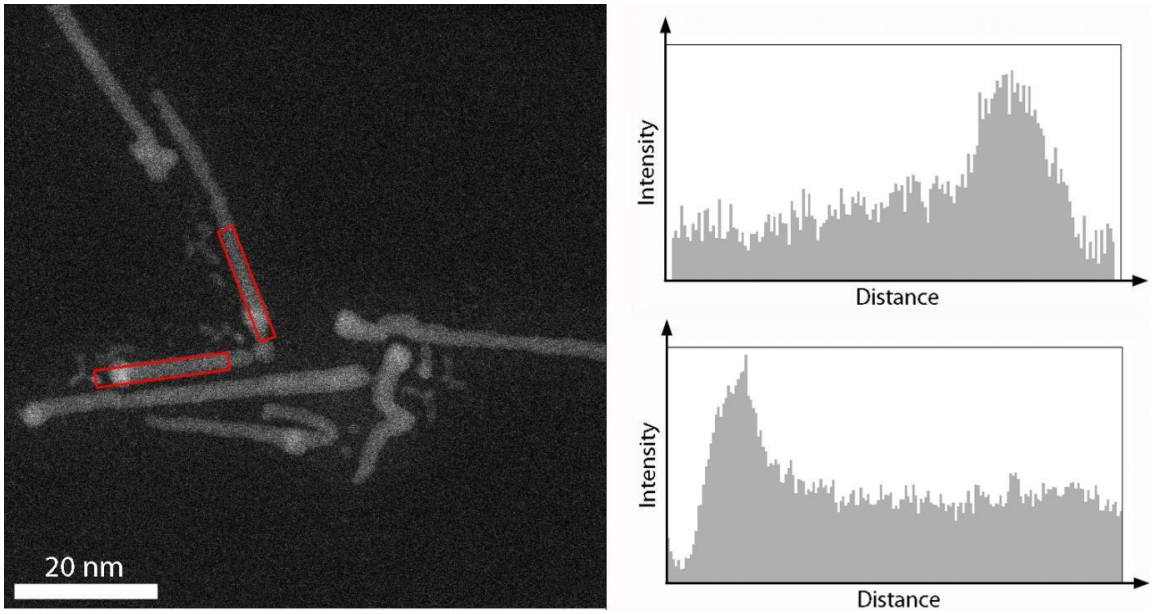

Figure S19. HAADF-STEM image of the CIS/ZnS HNCs. Both on sight as from the line profile, it is clear that one end of the nanorods has a higher intensity.

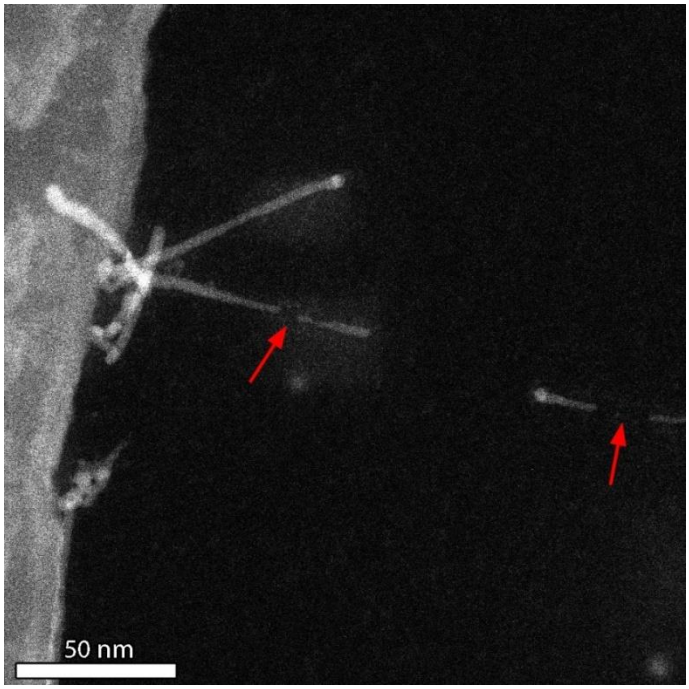

Figure S20. HAADF-STEM image of the CIS/ZnS HNCs after baking to reduce carbon contamination. It is clear that after baking some nanorods are broken.

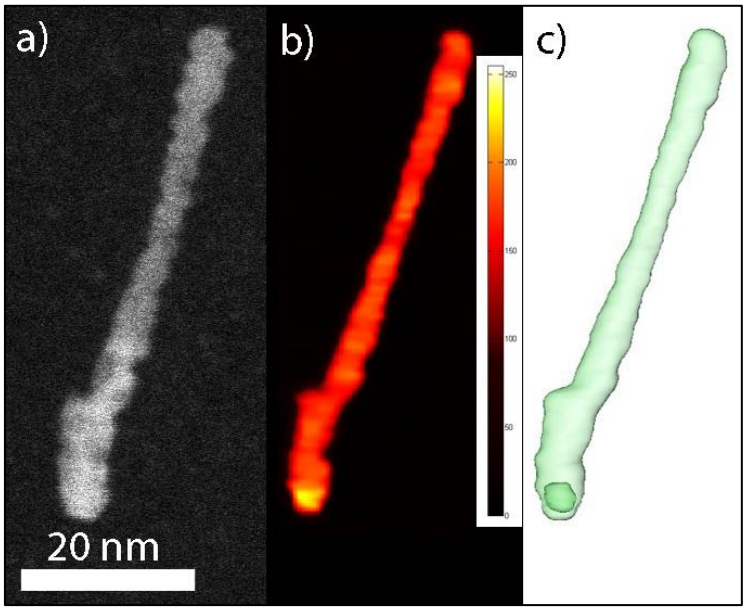

Figure S21. (a-b) 2D HAADF-STEM image and orthoslice through the reconstruction of a misformed CIS/ZnS dot-in-rod HNCs. The core appears brighter in the 2D image and the orthoslice. **(c)** A threshold is used to distinguish the core from the shell in 3D.

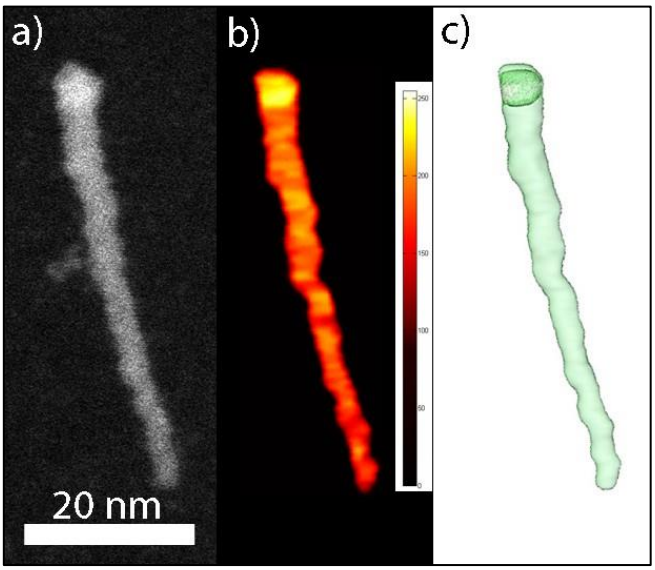

Figure S22. (a-b) 2D HAADF-STEM image and orthoslice through the reconstruction of a straight CIS/ZnS dot-in-rod HNCs. The core appears brighter in the 2D image and the orthoslice. **(c)** A threshold is used to distinguish the core from the shell in 3D.

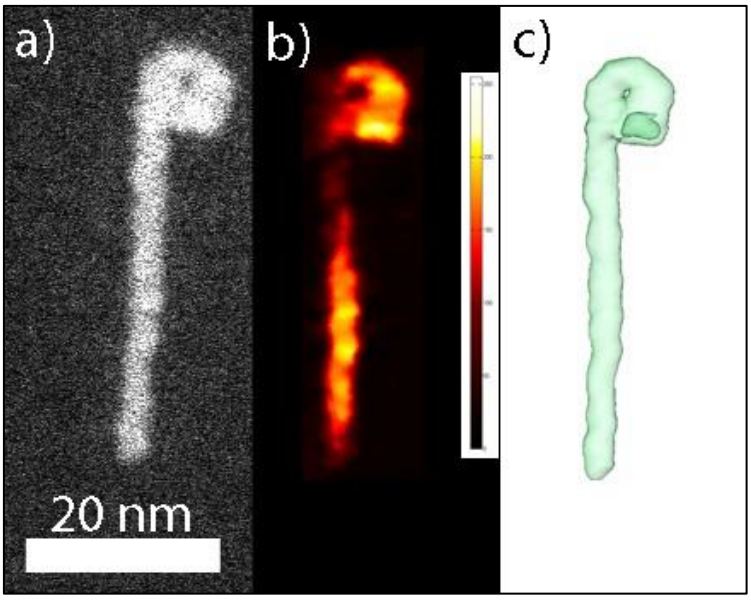

Figure S23. (a-b) 2D HAADF-STEM image and orthoslice through the reconstruction of a misformed CIS/ZnS dot-in-rod HNCs. The core appears brighter in the 2D image and the orthoslice. **(c)** A threshold is used to distinguish the core from the shell in 3D.

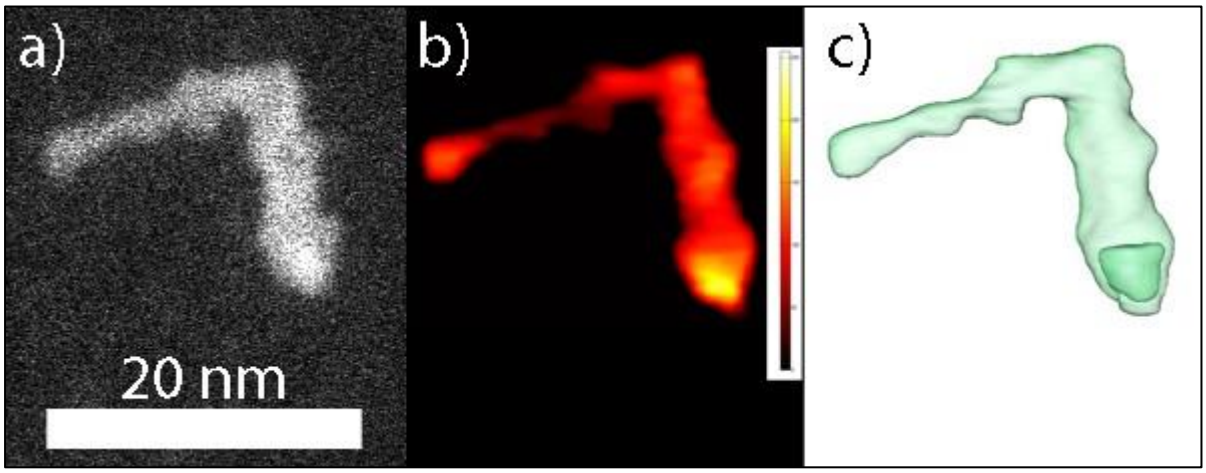

Figure S24. (a-b) 2D HAADF-STEM image and orthoslice through the reconstruction of a misformed CIS/ZnS dot-in-rod HNCs. The core appears brighter in the 2D image and the orthoslice. **(c)** A threshold is used to distinguish the core from the shell in 3D.

Crystal structure (JCPDS Card 01-077-9459)

Formula	$CuInS_2$
Crystal system	Wurtzite
Space group	P63mc (186)
Lattice parameters	a=b= 3.90652Å; c= 6.42896 Å; α =β=90 °; γ=120 °

Atomic Coordinates

Atom	Num	Wyckoff	Symmetry	x	y	z	SOF	IDP	AET
S	1	2b	3m.	0.33333	0.66666	0.0	1.0		
Cu	2	2b	3m.	0.33333	0.66666	0.3752	0.5		
In	3	2b	3m.	0.33333	0.66666	0.3752	0.5		

Crystal shape (**Obtained from HRTEM in Fig S13**)

NO.	h	k	l	d (Å)
1	0	-1	0	3.23
2	0	1	0	3.23
3	0	0	2	3.46
4	0	0	-2	3.46
5	-1	0	1	3.42
6	1	0	-1	3.42
7	0	-1	1	3.42
8	0	1	-1	3.42
9	-1	1	0	3.42
10	1	-1	0	3.42

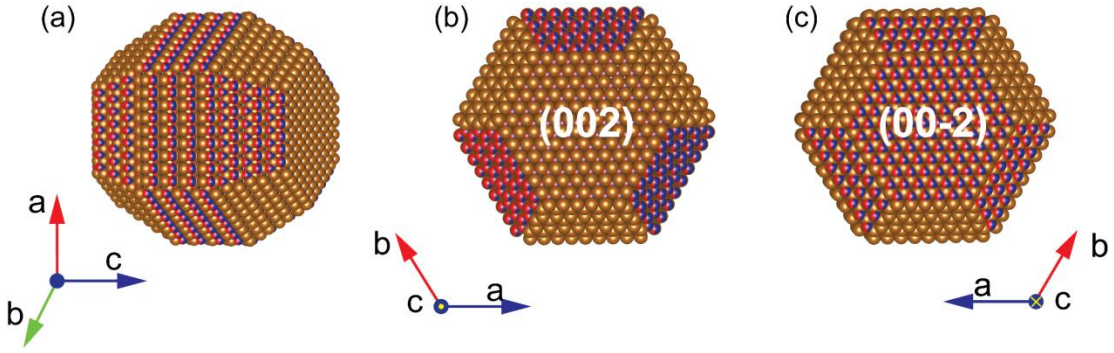

Figure S25. Crystal shape of CIS NCs. (a) perspective view, (b) [001] projection, (c) [00-1] projection

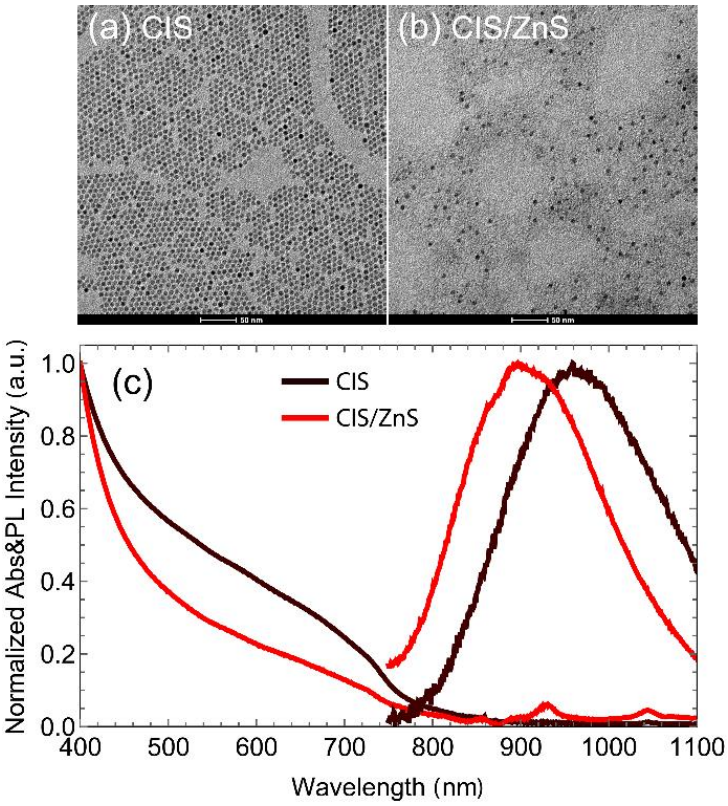

Figure S26. (a-b) TEM images of DDT capped CIS QDs **(a)** and product NCs **(b)** obtained from a seeded growth reaction in which the NCs shown in (a) were used as seeds. The reaction conditions were the same as used for the seeded growth reactions discussed above (method IV). **(c)** Absorption and PL spectra of the DDT capped CIS QDs shown in (a) and the product NCs shown in (b). The DDT capped CIS QDs used as seeds were synthesized by partial Cu^{+} for In^{3+} cation exchange in 5.6 nm template $Cu_{2-x}S$ NCs at 125 ˚C, following previously reported procedures (*Chem. Mater.* 2017, **29**, 4940−4951).

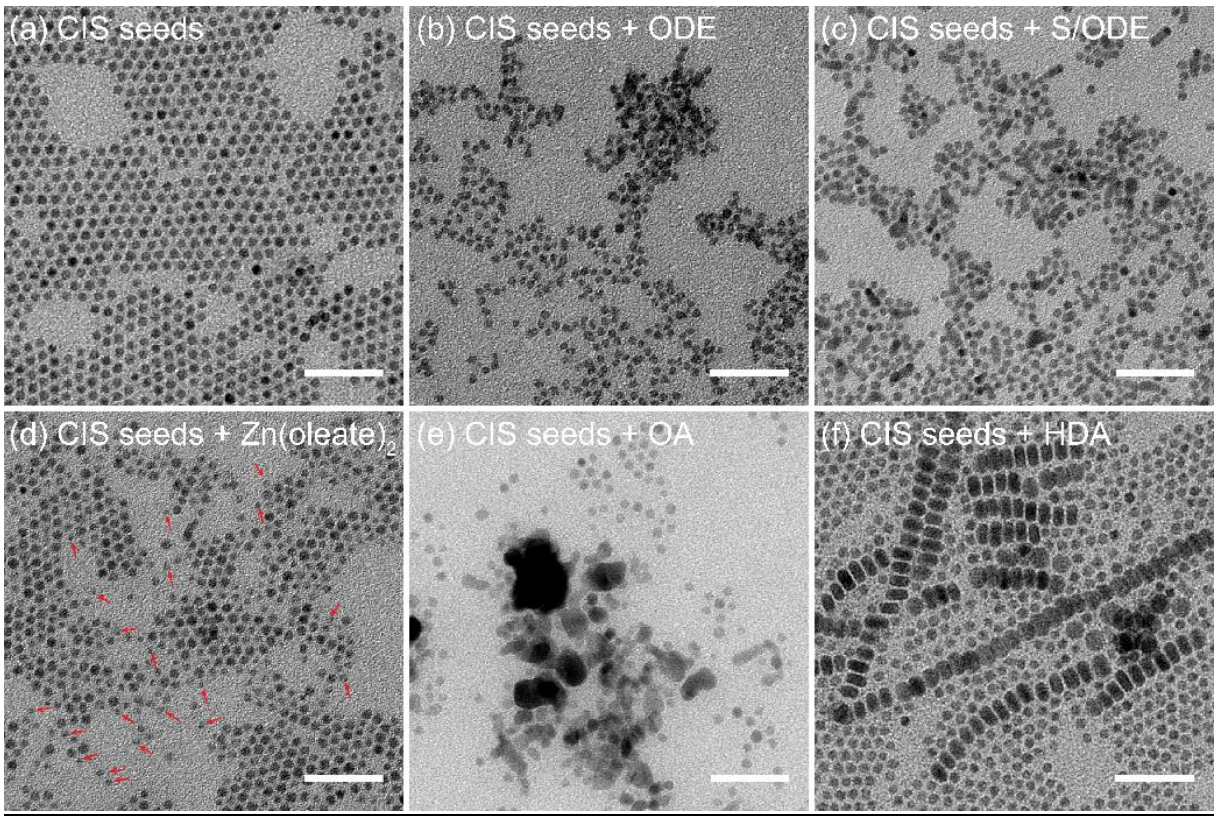

Figure S27. TEM images of CIS seed NCs (100 μL of a solution of 5.68×10^{-6} mmol CIS NCs in Octadecene) **(a)** prior to and **(b-f)** after 10 min in a hot (210 ˚C) solution containing 0.1 mmol of different ligands in 5 ml of Octadecene (ODE): **(b)** No ligands (ODE only); **(c)**. Sulfur in ODE (S/ODE); **(d).** Zinc oleate ($Zn(oleate)_2$); **(e).** Oleic acid; **(f).** Hexadecylamine (HDA).

Supporting method 1: Determination of CIS NCs concentration.

From ICP measurements, the Cu^+, In^{3+} and S^{2-} concentration in product CIS NCs are 0.0582 mmol/ml, 0.027 mmol/ml and 0.0716 mmol/ml, respectively. The product CIS NCs are wurtzite structure. In this hexagonal close packing, each unit cell possesses 2 cations (Cu^+ or In^{3+}) and 2 anions (S^{2-}). To simplify NC concentration calculation, we approximate the Cu/In ratio to 1. If the NC concentration is determined by Cu^+, then the NC concentration is deduced as follows:

As the diameter (d) of the CIS NC seeds is 5.5 nm, the volume of a single NC is:

$$V_{single\ CIS} = \frac{4}{3}\pi(\frac{d}{2})^3 = \frac{4}{3}\pi(\frac{5.5}{2})^3 = 87.1137\ nm^3 = 8.71 \times 10^4\ Å^3$$

The unit cell volume of wurtzite CIS NCs is:

$$V_{unit\ cell} = a^2c \cdot \sin 60^\circ = \frac{\sqrt{3}}{2}a^2c = 84.99\ Å^3$$

The number of unit cell per NC is:

$$N_{unit\ cell} = \frac{V_{single\ CIS}}{V_{unit\ cell}} = \frac{8.71\times10^4 Å^3}{84.99\ Å^3} = 1024.83$$

The number of Cu atoms in each unit cell is:

$$N_{Cu\ in\ unit\ cell} = 2 \times 50\% = 1$$

The number of Cu atoms per NC is:

$$N_{Cu\ singe\ CIS} = N_{unit\ cell} \times N_{Cu\ in\ unit\ cell} = 1024.83$$

Since the Cu^+ amount of 1ml of product NCs is:

$$n_{cu+} = 0.0582\ mmol$$

The amount of NCs in 1 ml solution is:

$$n_{NCs} = \frac{N_A n_{cu+}}{N_A N_{Cu\ singe\ CIS}} = \frac{0.0582\ mmol}{1024.83} = 5.68 \times 10^{-5} mmol$$

Therefore, the CIS NC concentration is 5.68×10^{-5} mmol/ml.

Supporting method 2: Measuring the photoluminescence quantum yields (PLQYs):

Lumogen red 305 (PLQYs=95% in toluene) was chosen as the standard dye due to its better PL overlap and appropriate excitation peak (442 nm) with CIS-based NCs compared with some other commercial dyes (*e.g.* Rhodamine B, Rhodamine 101, Rhodamine 6G). The PLQYs were calculated according to the following equation:

$$\emptyset_x = \emptyset_{ST} \frac{Gradx}{Grad_{ST}} \times \frac{n_x^2}{n_{ST}^2}$$

where the subscripts ***ST*** and ***X*** denote standard and sample respectively, ***Φ*** is the PLQYs, ***Grad*** the gradient from the plot of integrated PL intensity versus absorbance, and ***n*** the refractive index of the solvent. To reduce random error, five different concentrations of lumogen red 305 and NCs were measured.

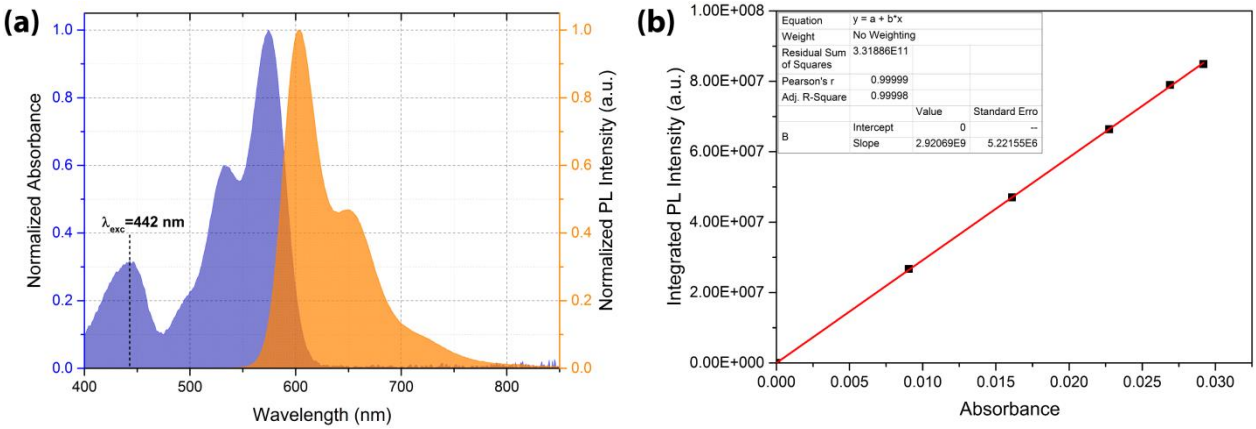

Figure S28. (a) Absorption (purple filled area) and PL (orange filled area, excitation wavelength= 442 nm) spectra of lumogen red 305 in anhydrous toluene. **(b)** Plotting of integrated fluorescence intensity versus absorbances of lumogen red 305 with 5 different concentrations. The gradient was obtained by linear fitting with intercept 0. The absorption and PL spectra of CIS-based NCs dissolved in toluene were measured under the same conditions.